ELSEVIER

Journal of Nuclear Materials 275 (1999) 255–267

journal of nuclear materials

www.elsevier.nl/locate/jnucmat

Hydride distribution around a blister in Zr–2.5Nb pressure tubes

G. Domizzi, G. Vigna*, S. Bermúdez, J. Ovejero-García

U.A. Materiales, Gerencia Centro Atómico Constituyentes, Comisión Nacional de Energía Atómica, Av. Libertador 8250, 1429 Buenos Aires, Argentina

Received 11 December 1998; accepted 25 May 1999

Abstract

Blisters were grown in Zr–2.5Nb pressure tube sections by a thermal gradient without applying external stress. The surrounding hydride distribution was analyzed. Hydride platelets were observed in the radial direction of the blister. The precipitation of these hydrides was found to be favored by low temperature of blister growth and slow cooling rate after blister formation. The misfit strain produced by hydride blister growth provides the stress necessary to promote radial precipitation. During the subsequent tensile test at 200°C (delayed hydride cracking test) the radial hydride length and thickness are increased. This increase is explained by a stress concentrator effect of the blister. When this effect vanishes, the increase of radial hydrides continues by an autocatalytic effect and stress concentrator effect of the hydride platelet. If a crack originated in the blister reaches the matrix it could propagate along a radial hydride previously precipitated.

1. Introduction

In 1983 a failure of a Zircaloy 2 pressure tube occurred in Pickering Unit 2 nuclear reactor. Due to the moving of a garter spring, a contact between the pressure tube and the cooler calandria tube was possible. Then the temperature gradient in the pressure tube wall caused the diffusion of hydrogen and deuterium to the cold point, initiating the formation of blisters. Some cracks in the blisters grew by delayed hydride cracking (DHC). When the crack reached the critical size a suddenly through-wall fracture, 2 m long, was developed in the axial direction [1].

After the Pickering event, several theoretical and experimental studies were made to analyze the blister formation in Zr–2.5Nb pressure tubes (PT). In the experimental works, blisters were grown under various conditions and different surrounding hydride distributions were reported. Puls [2] reproduced the cold spot by pressing a copper rod on the specimen. The blisters formed under this condition presented a 'sunburst' aspect, i.e., hydrides aligned in the radial direction of the blister emerging from the zone of high hydride density. In the same work, other blisters were grown in similar conditions but with a tensile stress applied along the circumferential direction of the tube (DHC test). Long strings of hydride platelets with their normals along the circumferential direction of the PT (hereafter named radial hydrides) were observed near the blister in the samples that did not fracture. Leger et al. [3] grew blisters both on small specimens and on pressurized sections of tubes. The cold spot in the first case was obtained by impinging a jet of compressed air upon the sample. Only platelets with their normal parallel to the radial direction of PT (hereafter named circumferential hydrides) were observed around the blisters grown by this method. On the contrary, the blisters grown in the pressurized tubes (plastically bent to contact the calandria tube) presented the sunburst aspect described above. Domizzi et al. [4] grew blisters with a cold finger refrigerated by water and pressed over the sample. These blisters did not present radial hydrides. During the subsequent analysis of the Pickering failure, several metallographic studies were

* Corresponding author. Tel.: +54-11 4754 7287; fax: +54-11 4754 7362.

E-mail address: vigna@cnea.gov.ar (G. Vigna)

0022-3115/99/$ - see front matter
PII: S0022-3115(99)00130-0

made on transversal sections of the blisters. They showed the presence of 'radiating spikes' hydrides in a zone of high hydride concentration surrounding the blister [1]. Moan and Rodgers [5] reported long radial hydrides in the matrix near the blister. They observed that some cracks, originated in the blister, had penetrated into the matrix and were associated to the radial hydrides.

On the other hand, a great deal of work was developed on DHC phenomenon in Zr–2.5Nb alloys. Excepting the above mentioned Puls's work, most of them used fatigue pre-cracked specimens with circumferential hydrides. Consequently the effect of radial hydrides on the propagation of a crack by DHC was not analyzed.

The fracture resistance of zirconium alloys is significantly reduced by the precipitation of hydride platelets oriented perpendicular to the applied stress [6]. As the main stress in pressure tubes is the hoop stress, precipitation of hydride strings in the radial direction must be avoided. Therefore, the fabrication route of Zr–2.5%Nb PT promotes the formation of hydrides with a circumferential–axial macroscopic habit plane [7]. Nevertheless, when the circumferential stress exceeds a threshold of ≈190 MPa (Leger [8]) the precipitation of radial hydrides is produced.

Due to the volume expansion, associated with the precipitation of zirconium hydride, stresses are produced in both the hydride blister and the surrounding zirconium matrix [9–12]. Some work [13–16] was made in order to calculate these stresses. In the matrix, near the axis of symmetry of an ellipsoidal blister, the models predict tensile stresses on the circumferential–axial plane. These stresses, added to compressive stresses along the radial direction of the blister, could overcome the threshold stress needed to precipitate radial hydrides.

The purpose of this work is to study the parameters that may affect the hydride distribution around the blister and to clarify the conditions that determine the precipitation of radial hydrides. The results of some blister growth tests, without external applied stress, are reported in Section 3.1 of this work. Some samples having blisters were exposed to the DHC test (Section 3.2). The changes that radial hydrides experiment during the application of an external circumferential stress were analyzed by metallographic observations. This analysis was made in the context of a more extensive work directed to study the effect of radial hydrides on the DHC process.

2. Experimental

2.1. General

The tests were made on specimens obtained from commercial Zr–2.5%Nb pressure tubes. In some samples (A, B, C) the outer and the inner surfaces of the tube were straightened by abrading with SiC paper. The dimensions of samples A and B were 14 mm, 10 mm and 3.3 mm in the circumferential, axial and radial directions, respectively, while samples C were $(40\times10\times2)$ mm^3 in size. One sample (F), $(33\times2.8\times3.6)$ mm^3 in size, was flattened by reverse bending and then was stress relieved at 400°C for 24 h.

All samples were hydrided by cathodic charge. This hydriding method produces the formation of a hydride layer on the sample surface. A heat treatment was carried out in some samples (A, C, F) in order to obtain a uniform hydride distribution throughout the volume (details are reported in Section 2.2).

A blister was grown on each sample by applying a thermal gradient (see Section 2.3). The blister dimensions and hydride distributions were observed by optical microscopy (see Section 2.4). Finally, DHC tests were carried out on sample F and the majority of samples C (see Section 2.5).

2.2. Hydriding and homogenization annealing

Previous to the hydriding, the samples were etched in a solution of 45 ml HNO_3, 45 ml lactic acid and 6 ml HF. The cathodic charge was performed in a 0.05 M H_2SO_4 solution. The current density was higher than 150 mA/cm^2 and the temperature was 90–98°C. The time of charging was long enough to assure a hydrogen content higher than the terminal solid solubility corresponding to the thermal treatment of homogenization.

Samples A, C and F were heat-treated to obtain a homogeneous hydride distribution. Subsequently the remaining hydride layer was removed with abrasive paper. The annealing treatments were made in vacuum. Samples A were annealed at (465 ± 5)°C during 19 h. After that, the samples were air-cooled to room temperature by removing the furnace and injecting air into the vacuum chamber. Samples C were heat treated at (380 ± 5)°C during 23 h and sample F was annealed at (400 ± 5)°C during 24 h. Samples C and F were cooled to room temperature in vacuum, out of the furnace.

Samples B were not thermally treated after the cathodic charge in order to have all hydrogen in solution around the blisters during their growth. The hydride layer was removed on the outer PT surface but not on the inner PT surface. The latter was thick enough to assure that it would act as a hydrogen source during blister growth.

2.3. Blister growth annealing

A localized thermal gradient was applied to each sample in order to form a blister on the outer surface of the PT. The experimental device was similar to that described in a previous work [4]. The sample was placed

over an aluminum squared block heated in an electrical furnace. The thermal gradient was obtained by pressing an aluminum cold finger on the upper surface of the sample. The contact area was 2.2 mm in the circumferential direction of the PT and 10 mm in the axial one.

To improve thermal conductivity, an 80-mesh aluminum powder was deposited between the sample and the cold finger and between the sample and the hot Al block. The temperature of the sample was measured with a J-type sheathed thermocouple placed inside the 5 mm deep holes. The holes were made by spark erosion, at $x = 0.5$ mm (from the lower surface in the radial direction) and $y = 6$–7 and 20 mm (in the circumferential direction, from the blister middle axis).

The temperature of the cold finger was measured in a similar way at 12 mm from its contact with the sample. The temperature of the sample, the testing time and the cooling rate were changed in the different tests (as is described in Section 3).

2.4. Metallography

In order to measure the blister dimensions and to observe the hydride distribution around it, the samples were progressively ground with SiC paper on the radial–circumferential plane. They were etched in a 45 ml HNO_3, 45 ml lactic acid and 6 ml HF solution.

Fig. 1(a) is a scheme of the metallographic section (radial–circumferential plane) of a blister showing its depth (a), diameter (d) and the protrusion height (h). The blister length (l) along the axial direction was measured on the outer surface. The distribution of the hydride particles growing in the radial direction of the blister (approximately parallel to the radial–axial plane of the PT) was characterized by measuring the particle length (L) and the reach (R). The reach was measured from the blister – matrix interface to the farthest radial hydrides. In samples A, B, and CQ these parameters were measured after successive grindings. The values corresponding to the middle of the blister are reported. This was not possible in samples C1–C5 because they would be used to prepare tensile specimens for the DHC test, so the observation was carried out at 2 mm from the middle. Nevertheless, the experience obtained from samples A, B and CQ allows us to assure that the above mentioned parameters do not change appreciably in a range of 2 mm from the middle of the blister.

2.5. Delayed hydride cracking test

After the blister growth samples C1–C4 were machined to obtain tensile specimens (Fig. 1(b)). In the axial PT direction the thickness was reduced to 4 mm in a gage length of 10 mm (circumferential direction). The tensile axis was coincident with the PT circumferential direction.

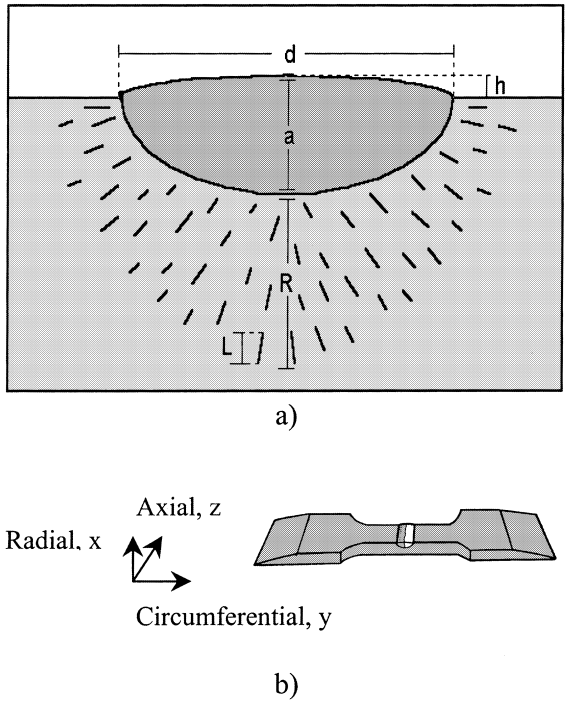

Fig. 1. (a) Scheme of the circumferential–radial section of a blister and distribution of hydride particles in the radial direction of the blister. (b) Scheme of the tensile specimens C with a cracked blister.

Cracks are always observed inside the blisters. Usually, these cracks do not reach the surrounding matrix. Then, it is not sure that they can propagate by DHC. Therefore, previous to the DHC test, the sample was bent in a three-point device to assure that a crack comes in the matrix. A static load was applied without surpassing the matrix yield stress. After loading, the propagation of the cracks was observed, on both sides of the sample, by optic microscopy. The load was incremented just to a point in which a crack crosses the region of high hydride density (which usually surrounds the blister). Then, during the DHC test, the initial depth of the crack can be considered similar to the blister depth.

After machining the tensile specimens, the depth of the blister was uniform along the axial direction (this was verified after the specimen fracture). Consequently, the bending test caused the depth of the crack being uniform too (through-wall cracks), so the stress intensity factor, K_I, can be calculated using the formula corresponding to a single notched specimen:

$$K_I = \frac{P\,Y}{B\,W^{1/2}},$$

$$Y = 1.99\left(\frac{a^*}{W}\right)^{1/2} - 0.41\left(\frac{a^*}{W}\right)^{3/2} + \cdots, \qquad (1)$$

where P is the load, W measured in the radial direction and B in the axial direction, a^* is the depth of the crack after the bending test [17].

The tests were carried out in a statically loaded creep-testing machine. The specimens C were heated to 280°C, held for 1 h, and then cooled to 200°C. Then they were subjected to dead loading and the time to failure was measured, excepting sample C2 which was unloaded after 48 h and air cooled.

After sample fracture, one of the sections was mounted in an EPOMET molding compound to protect the fracture surface. Then it was etched to observe the hydride distribution on the radial–circumferential plane. On the other section, the fracture surface was observed by scanning electron microscopy (SEM).

Due to the dimensions of sample F, it was not possible to machine a tensile specimen with the shape shown in Fig. 1(b). To hold the sample, holes were machined at the ends. To avoid the fracture through the holes, the specimen width was smoothly reduced from 2.8 to 2 mm in the middle length. The specimen was loaded, then heated to 300°C, held for 1 h and cooled to 212°C, after 940 h it was unloaded and air-cooled.

3. Results: analysis and discussion

The different hydride distributions obtained after blister growth are presented in three groups (Section 3.1) according to the parameters of blister growth: cooling rate, temperature of blister formation and previous hydride distribution. In Section 3.2 the observations after the DHC test are reported.

3.1. Blister growth

In samples A, C and F the homogenization annealing produced the precipitation of circumferential hydrides, as usual in PT. During the blister growth, these circumferential hydrides did not completely dissolve near the cold finger. Therefore, after cooling, a region with

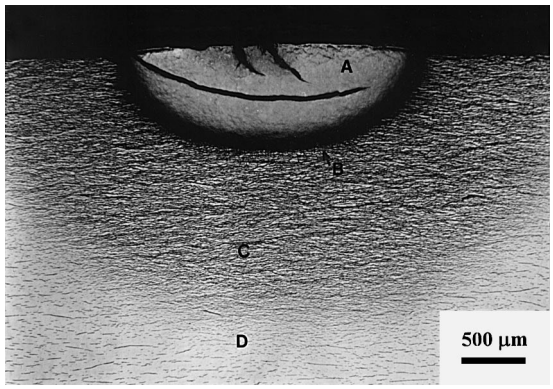

Fig. 2. Circumferential–radial section of a sample A. The blister (A) is surrounded by a region of high hydride density (B), then by a region of non dissolved previous circumferential hydrides (C) and finally by the region where hydrogen was in solution (D). Cracks are observed inside the blister.

circumferential hydrides, like the previous ones, is observed near the blister. The region where all the hydrogen was in solution (during blister growth), can be seen in Fig. 2.

Examination of the sample surface showed that all the blisters presented cracks after the growth test. Usually, the cracks (on the radial–axial plane) were interconnected by some branches in the circumferential direction. The micrographs of the circumferential–radial plane (Fig. 2) shows that radial–axial cracks remained inside the blister. Other internal cracks (on the circumferential–axial plane) were also observed.

3.1.1. Effect of the cooling rate

In samples C the blisters were grown under the same conditions of temperature and time (Table 1) but under different cooling rates, as shown in Fig. 3(a). With the cold finger applied, samples C1 and C4 were cooled in covered furnace; instead, sample C2 was cooled in open furnace to 368°C, and forced convection was used from this temperature to room temperature. Samples C3 and

Table 1
Blister growth conditions and length of radial hydrides in samples subjected to the cooling rates shown in Fig. 3

Sample	Temperature at (x, y) (°C)			Time (days)	Blister dimensions[a] (mm)		Radial hydrides length (μm)
	(14, 0)	(0.5, 7)	(0.5, 20)		d	a	
C1	75	386	396	14	2	0.5[b]	<100
C4	69	390	400	14	2	0.5[b]	<100
C2	70	388	396	14	1.5	0.5[b]	<80
C3	75	387	396	14	1.9	0.5[b]	<50
C5	72	388	395	14	2.5	0.5[b]	<40
CQ	63	388	398	14	2.4	0.8	No radial hydrides (sunburst <80 μm)

[a] Blister dimensions: depth (a), diameter (d), see Fig. 1.
[b] Measured at 2 mm from the middle of the blister, along axial direction.

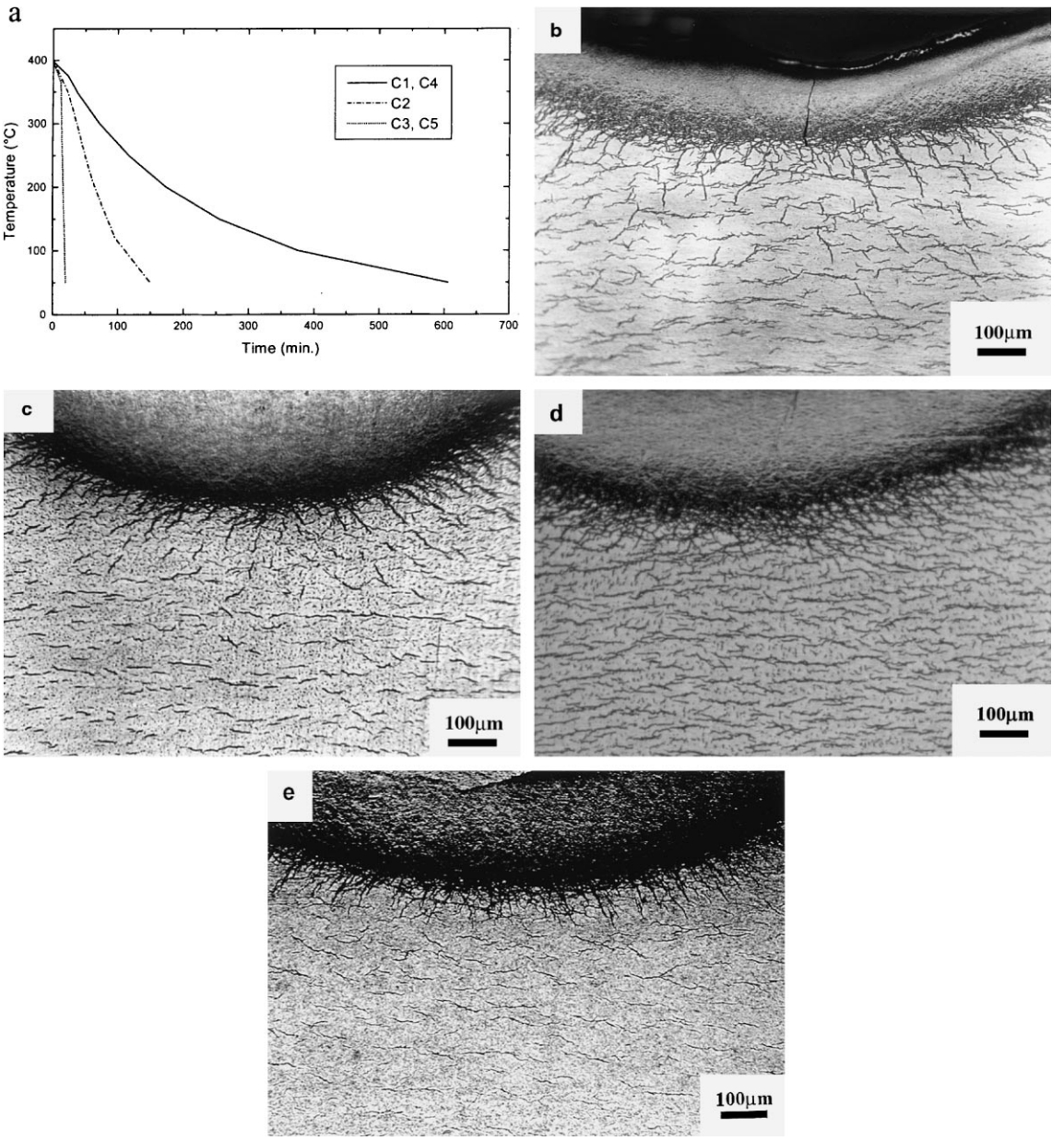

Fig. 3. Effect of the cooling rate on the radial hydride length. (a) Curves of cooling after blister growth. (b)–(e) Micrographs of samples C1, C2, C3 and CQ, respectively. In the latter, only the sunburst effect is observed.

C5 were cooled in the same condition as sample C2 to 368°C, then they were removed from the furnace and cooled in air to room temperature.

Micrographs of the circumferential–radial section of samples C1, C2 and C3 (at 2 mm from the middle of the blister) are shown in Fig. 3(b)–(d). All samples presented hydrides, in the matrix around the blister, grown in the radial direction of the blister. Some of them lay in the blister/matrix interface and produced a hydride distribution similar to the 'sunburst' reported by Puls [2]. Others (named radial hydrides) have precipitated near the blister (Fig. 1(a)) and between the previous circumferential hydrides.

No external stress was applied during blister growth. Then, the stress necessary to overcome the threshold stress [8] and precipitate radial hydrides must be attributed to the misfit strain produced by the blister formation.

The blister dimensions and the length of radial hydrides are reported in Table 1. The radial hydride length

Table 2
Effect of the blister growth temperature on the reach of radial hydrides. During blister growth, samples A had circumferential hydrides precipitated. Samples B had a surface hydride layer, being hydrogen in solution inside the samples

Sample	Temperature at (x, y) (°C)[a]		Time (days)	Cooling conditions	Blister dimensions[b] (mm)				Radial hydrides (μm)	
	(15,0)	(0.5,6)			d	a	h	l	L	R
AQ	60	352	14	Water quenched	2.64	0.98	0.12	6.3	No radial hydrides	
A4	60	317	32	Covered furnace	2.68	0.96	0.09	3.9	30	500
A2	60	352	14	Covered furnace	2.66	1.03	0.12	5.0	18	410
A5	61	376	12	Covered furnace	2.71	0.91	0.14	4.6	0	0
B4	67	293	60	Covered furnace	2.93	1.04	0.12	3.87	80	400
B1	70	321	30	Covered furnace	3.1	1.2	0.15	5.5	50	180
B2	73	353	14	Covered furnace	2.65	0.96	0.10	5.3	0	0
B3	73	353	14	Covered furnace	3.1	0.88	0.12	4.5	0	0

[a] Reported values were measured at the beginning of the test.
[b] Blister dimensions: diameter (d), depth (a), protrusion height (h), and length in the axial direction (l). Radial hydride: particle length (L), reach (R).

increases as the cooling rate decreases. This may be considered as an indication that the radial hydrides precipitated and grew during cooling by a hydrogen diffusion process.

To corroborate that they were not present at the temperature of blister growth, two samples (CQ and AQ) were water-quenched. In this way, the cooling rate was high enough to prevent the hydrogen diffusion. Then, the growing of radial hydrides (if they were precipitated) could be prevented during cooling after the blister formation.

In both samples, the so-called radial hydrides were not observed at all. This confirms that (when no external stresses are present) they do not precipitate at the temperature of the blister formation, but during subsequent cooling if the hydrogen diffusion is allowed. The cooling provides the supersaturation necessary to produce their precipitation. In sample CQ only the sunburst effect was found (Fig. 3(e)), these hydrides precipitated beside the blister boundary while the blister was growing. The conditions of blister growth of sample CQ are presented in Table 1 and those of AQ can be seen in Table 2 together with another samples A that will be discussed in Section 3.1.2.

3.1.2. Effect of the temperature

Blister growth tests were made at different temperatures and the time was modified to obtain a similar blister size. The results of samples A4, A2 and A5 are shown in Table 2 and Fig. 4(a)–(c). Sample A5 exposed to the highest temperature showed no radial hydrides. On the contrary, the blisters in samples A4 and A2, grown at lower temperature, are surrounded by hydrides precipitated along the blister radial direction. Moreover, the reach of radial hydrides (R) decreased with the increase in test temperature.

The elastic stresses inside the matrix, produced by the blister growth, decrease with the distance measured from the blister/matrix boundary (as it is predicted in the models of different authors [13–16]). The radial hydrides precipitate as far as these stresses exceed the threshold stress [8]. The fact that the reach of the radial hydrides was shorter when the temperature was higher is associated to the decrease of the yield stress with temperature. The higher the yielding of the matrix the lower the stresses developed around the blister. This temperature effect explains the absence of radial hydride surrounding the blisters grown at 390°C in tests made by Domizzi et al. [4].

The results of samples B are also shown in Table 2. The blisters in B4 (formed at 293°C) and B1 (formed at 321°C), presented some radial hydrides (Fig. 4(d)). In samples B2 and B3, the blisters grown at higher temperature (353°C) presented no radial hydrides.

Again, a temperature effect on the reach of radial hydrides was observed as discussed above. Nevertheless, the reach of samples B was shorter than the reach of samples A grown at similar temperatures, the reason of this result being yet not clear. A possible explanation is the following. Samples B (without homogenization annealing) had no circumferential hydrides during the blister growth. On the contrary, in samples A the radial hydrides grew between the previous circumferential ones, as it is observed in Fig. 4(a) and (b). Stresses are created during hydride precipitation (due to misfit between precipitate and matrix) and can be estimated for the case of platelet shaped hydrides. Chiu [18] calculated the stress field produced by a cuboid surrounded by an infinite elastic space. In the matrix, the stress component normal to the platelet plane is compressive, in the center of the platelet. These compressive stresses could then facilitate the precipitation of another platelet normally to the previous one. Then the stresses produced by the precipitation of previous circumferential hydride may reinforce the stresses produced by the blister formation resulting in a longer reach of radial hydride.

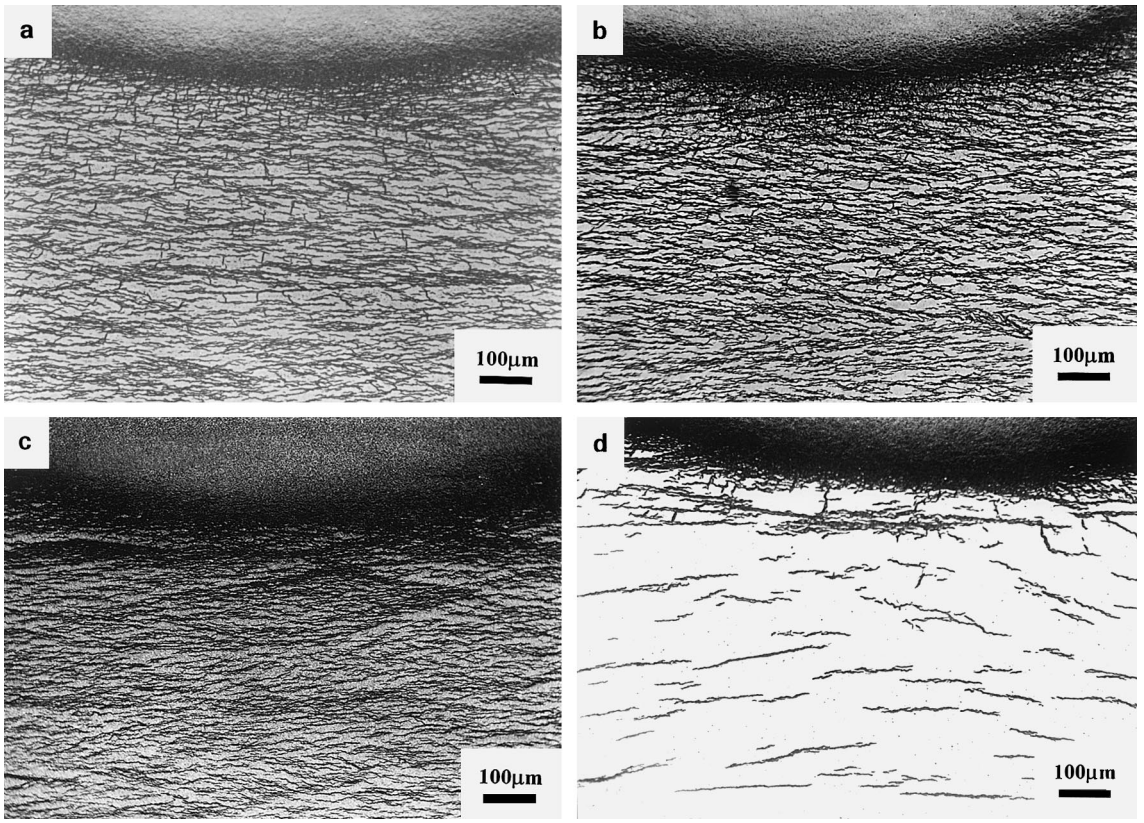

Fig. 4. Effect of the temperature of blister growth annealing on the radial hydride reach. (a) Sample A4 ($T = 317$°C), (b) sample A2 ($T = 352$°C), (c) sample A5 ($T = 376$°C) and (d) sample B1, without previous hydrides ($T = 321$°C).

3.1.3. Effect of the previous hydride distribution

As discussed above the presence of circumferential hydride during the blister formation affects the reach of radial hydride. On the other hand, the length of these hydrides is limited by the circumferential ones as can be seen comparing samples C and A.

Samples C had a similar previous hydride distribution (Fig. 5(a)) and the hydrogen concentration, corresponding to the terminal solid solubility at 380°C, was 171 ppm [19]. The hydrogen concentration of samples A was 460 ppm according to the homogenization treatment at 470°C. Then the distribution of circumferential hydrides in samples A was more compact (Fig. 5(b)) than the corresponding one to samples C. The same effect can be seen comparing Fig. 3(b)–(e) and Fig. 4(a)–(c) where the distribution of circumferential hydrides (surrounding the blister) is very similar to the initial one. The average distance between circumferential hydrides was 14–22 μm in samples A with a maximum distance of 40 μm, while in samples C the average was 50–60 μm and the maximum was 100 μm.

All samples A showed radial hydrides of similar size (18–30 μm) but shorter than those found in samples C1 and C4 cooled at the same rate (100 μm), as it is evident from comparing Tables 1 and 2 and Figs. 3 and 4. The reason of this difference may be attributed to the previous circumferential hydride distribution: the network of circumferential hydrides has limited the growth of the radial hydrides.

3.2. Delayed hydride cracking

The conditions and results of the DHC test are shown in Table 3. The results of specimens C are discussed in Section 3.2.1, these specimens were characterized as having a through-wall crack. The specimen F will be analyzed in a separate section (Section 3.2.2), because it presented a non through-wall crack.

3.2.1. Samples C

Specimens C1, C3 and C4 were dead-loaded and the time to failure was measured. Then the fracture surface was observed by SEM. All samples presented the same characteristics. Three zones are evident (Fig. 6): the first corresponding to the brittle fracture of the blister. The second appears as mainly brittle fracture, typical of the DHC test. The third corresponds to the ductile fracture of the matrix by overloading. A lower bound crack

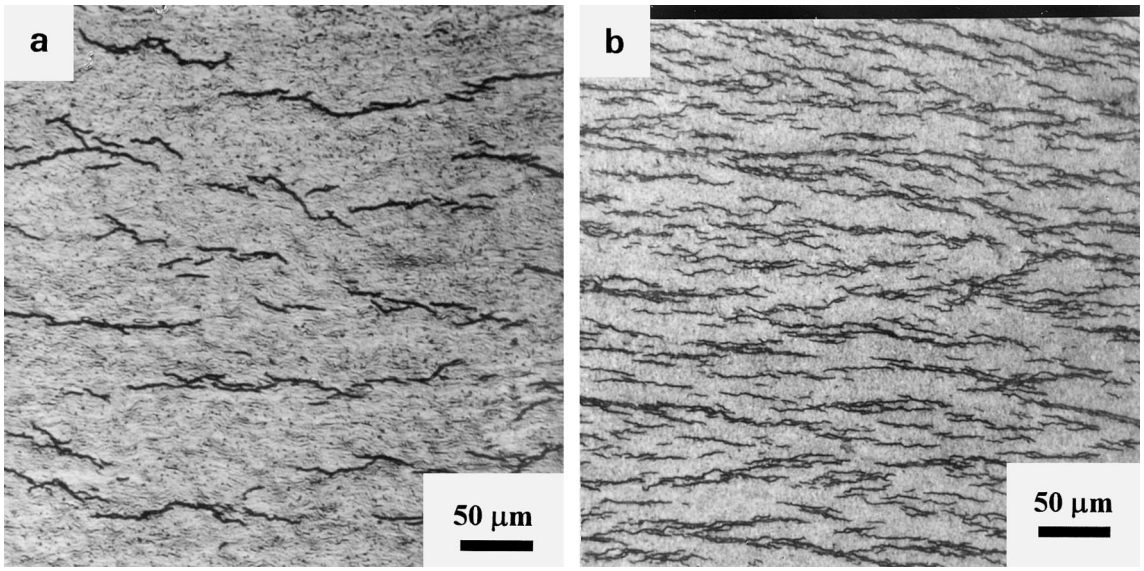

Fig. 5. Hydride distribution after homogenization treatment and before blister growth annealing. (a) Samples C, (b) samples A

Table 3
Conditions of the delayed hydride cracking tests[a]

Specimen	B (mm)	W (mm)	a^* (mm)	P (N)	σ (MPa)	K_{IH} (MPa m$^{1/2}$)	Time[b] (h)	v_C (10^{-9} m s^{-1})
C1	3.9	2.01	0.47	1618	204	8.8	119.0	2.5
C3	3.9	2.13	0.55	1519	183	8.5	78.4	4.0
C4	3.8	2.2	0.36	1904	228	8.6	38	9.8
C2	3.1	2.0	0.50	1176	190	8.4	48[c]	
F	2.0	3.6	0.14–1.0[d]	1078	150	3.5–9.4	940[c]	

[a] σ is applied stress; B, W, a^*, P, K_{IH} are described in the text.
[b] Loading time.
[c] Removed before fracture.
[d] Non-uniform crack along axial direction.

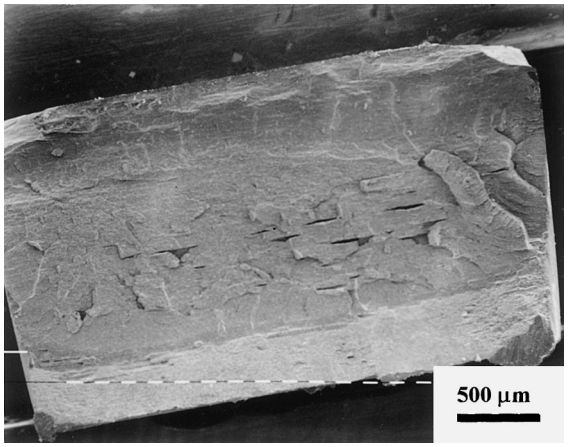

Fig. 6. Typical fracture surface of samples C after DHC test. Three zones are observed: the initial crack in the blister (top of the figure), crack propagation by DHC (middle), final ductile fracture (bottom of the figure).

velocity (v_C) was calculated from the test duration and the length of the DHC zone. The obtained values, reported in Table 3, ranged between 2.5 and 9.8×10^9 m s^{-1}. DHC tests, with the crack growth on the axial radial plane, were reported by Coleman and Ambler [20] and Ambler [21]. At 200°C and K_I values in the range where v_C is independent of K_I they measured a radial crack velocity of 3×10^{-9} m s^{-1} and 9.9×10^{-9} m s^{-1}, respectively.

Fig. 7 shows a micrograph of the circumferential–radial plane of sample C1 after the DHC test. The hydrides aligned in the radial direction of the blister presented length and thickness up to 250 and 10 μm, respectively. A comparison with the dimensions previous to the DHC test shows that an increase has occurred. The same observations are valid for specimen C3, but the maximum hydride length was 150 μm and the thickness was 4 μm. Being the temperature uniform throughout the sample, the driving force for hydrogen diffusion (and subsequent hydride growth) must be

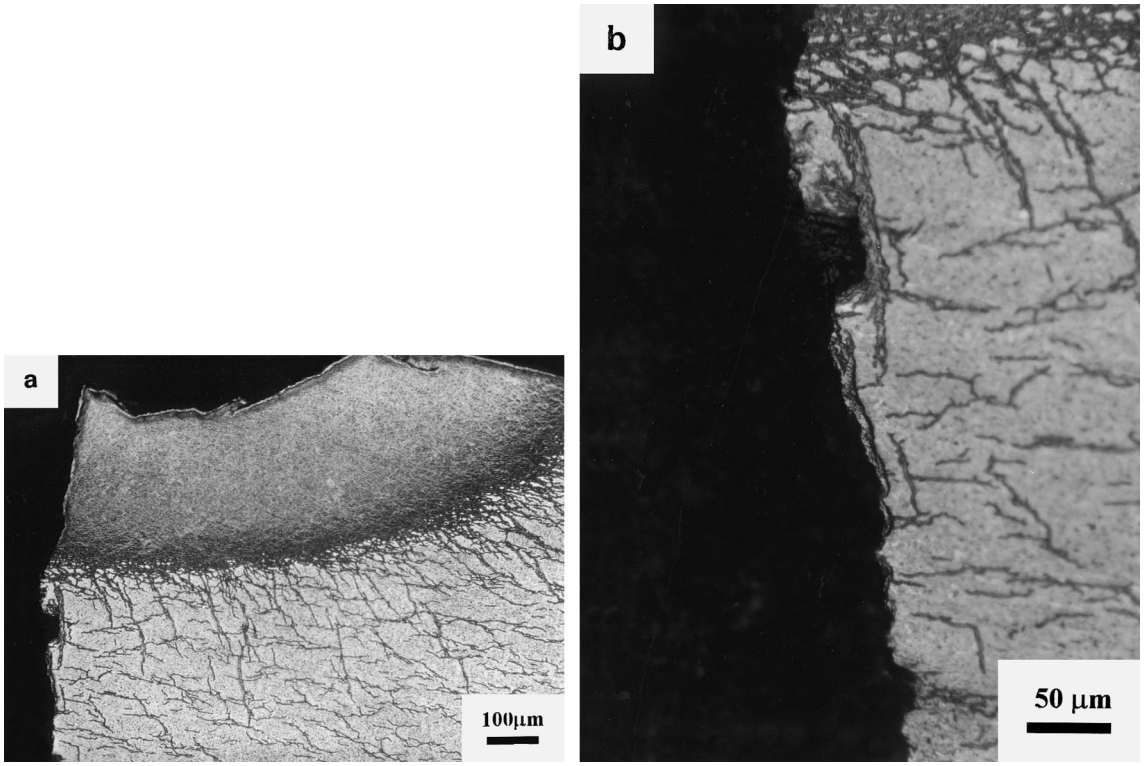

Fig. 7. Circumferential–radial plane of specimen C1 after DHC test: micrographs of a section normal to the fracture surface. (a) The blister and the surrounding hydride distribution are observed. (b) Amplified view showing radial hydrides along the fracture surface.

looked up in the stress gradient. It is known that cracks are important stress concentrators and produce the migration of hydrogen and hydride precipitation at the crack tip. Nevertheless, it is hard to believe that they could produce the growth of hydrides around the blister as far as 1000 μm from the crack tip (Fig. 7(a)).

As it was evident from the previous sections, in absence of external stresses, the blister produces stresses in the matrix that are high enough to induce the precipitation of hydrides radially to the blister. With the application of external tensile stresses the blister would act as a stress concentrator and the tensile stresses around it would be reinforced. In order to clarify this point sample C2 was tested. In this specimen the crack remained arrested in the blister even after the bending test (Fig. 8(a)). The DHC test was interrupted before cracking, the load was removed and the sample was quickly air-cooled. To observe the evolution of radial hydrides on the circumferential–radial plane, the surface oxide was removed by polishing with 1200 grit SiC paper. The metallography showed that the crack could not cross the region of high hydride density (Fig. 8(b)), probably because the applied tensile stress could not overcome the compressive stresses on the crack tip, inside the blister and near its boundary as predicted by Wallace [15]. Consequently, the crack could not act as a stress concentrator, nevertheless the length of radial hydrides increased from 80 to 200 μm as can be seen comparing Fig. 8(a) and (b). The reach of radial hydride increased too from 200 to 270 μm. This increase must be attributed to the increase in the length of the pre-existing radial hydrides rather than to the precipitation of new ones. These results were corroborated by the authors in other work [22] and they show that the blister acts as a stress concentrator when an external stress is applied. The stress gradient, generated around the blister, provides the hydrogen flow and the supersaturation necessary for the growth of radial hydrides. An autocatalytic nucleation of hydrides cannot be set aside, as it will be discussed in the next point.

On the other hand, in sample C1 just below the blister, a radial hydride is observed along the fracture surface (Fig. 7(b)). In DHC test reported by other authors the precipitation of hydride particles at the crack tip was observed, but their aspect is slightly different [23]. In the present case it is not quite clear whether the hydride had precipitated at the crack tip (as usual in DHC tests) or the crack has propagated along a previous radial hydride. An argument in favor of the latter possibility is that no radial hydrides were found along the crack away from the blister, out of the reach of radial hydrides. In addition, in sample C3 which had

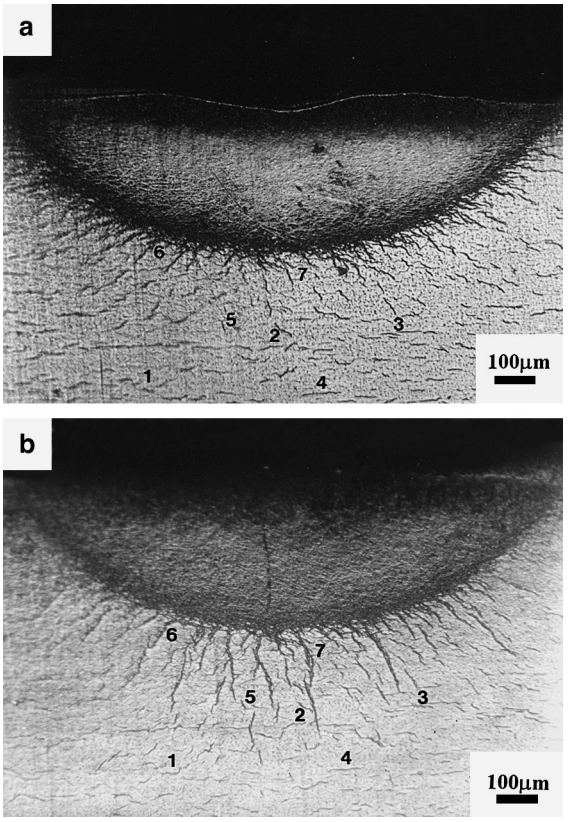

Fig. 8. Hydride distribution around the blister in sample C2. (a) Before DHC test. (b) After DHC test, the photograph shows the same surface that (a), after soft polishing with 1200 SiC paper and etching to remove the surface oxide. Some hydride particles are pointed out in both photographs in order to show that a negligible material layer was removed. Nevertheless, the radial hydride lengths present a noticeable increase.

shorter radial hydride than C1 the hydrides observed along the fracture near the blister were shorter too.

Nevertheless, it is interesting to note that if the radial hydrides have some effect on the propagation of the crack this effect ceases when the crack exceeds the reach of the radial hydrides. More tests are necessary to establish whether the blister and the radial hydride distribution have any effect on the crack rate in through wall-crack specimens.

3.2.2. Sample F

Prior to the DHC test of sample F, the metallography of the radial–circumferential plane on one side (hereafter named A) showed a crack (C_A) 1000 μm long that crossed the blister boundary and reached the matrix. On the other side (B) only a 140 μm long crack was observed which remained inside the blister. Both cracks extend along the axial direction as it was verified observing the free surface of the blister, but not through all the thickness. Hence, sample F was characterized for having a non-uniform crack along the axial direction, and the value of K_I was lower than K_I of samples C. This fact can explain that the specimen remained 940 h without failure (Table 3).

After removing the specimen from the creep machine, both sides were observed again. On side A the crack (C_A) had advanced up to 2185 μm from the sample surface in the radial direction of PT. After etching it was evident that the crack is associated with a string of hydrides (Fig. 9(a) and (b)). Furthermore, a non-cracked hydride string (H_A, 1000 μm long) had grown parallel to the crack.

The metallography of side B showed that the crack had propagated inside the blister but did not cross the blister boundary. As it was observed on side A, a hydride string 500 μm long (H_B) had precipitated along the radial direction of the PT. Successive polishings were made on this side. After removing 1 mm it was observed that another crack (C_B) had propagated along a hydride string radially to the blister (Fig. 10).

Consecutive polishing was carried out on the circumferential–axial plane beginning at the inner surface of the PT. Fig. 11 shows the section at 1.8 mm from the outer surface. Two long strings of hydrides are observed in the axial direction, each one corresponding to the radial strings observed on sides A and B (H_A and H_B). These observations evidence that extended stackings of radial–axial platelets have precipitated throughout the axial direction of the specimen. These axial–radial stackings of platelets remained uncracked in spite of their large dimension (≈1000 μm in the axial and radial directions).

It is known that the hydride platelets (observed by optical microscopy) are conformed by the stacking of sub-units precipitating in the stress field of the predecessors (autocatalytic nucleation) [7,24]. In a similar way, amplified observation of the mentioned macroscopic stackings revealed that they are formed by a succession of hydride platelets that were precipitated in steps. Each platelet is localized in a plane parallel to the preceding one and their tips are overlapped (Figs. 10 and 11). The stackings of platelets observed in sample F are similar to those shown in Puls' work [2] in the specimens not cracked after the DHC tests. The platelets are first radially oriented to the blister, denoting that they precipitate normally to the stresses produced by the blister (misfit strain and stress concentrator effects of the blister). Then, when these stresses vanish, the platelet stacking grows along the radial direction of the PT, i.e., normally to the external stress, impelled by the autocatalytic nucleation and the stress concentrator effect of the platelet itself under the external stress.

Sample F and samples of Puls' work were obtained from flattened PT, the flattening procedure originates a pattern of residual stresses through the specimen [8]. In

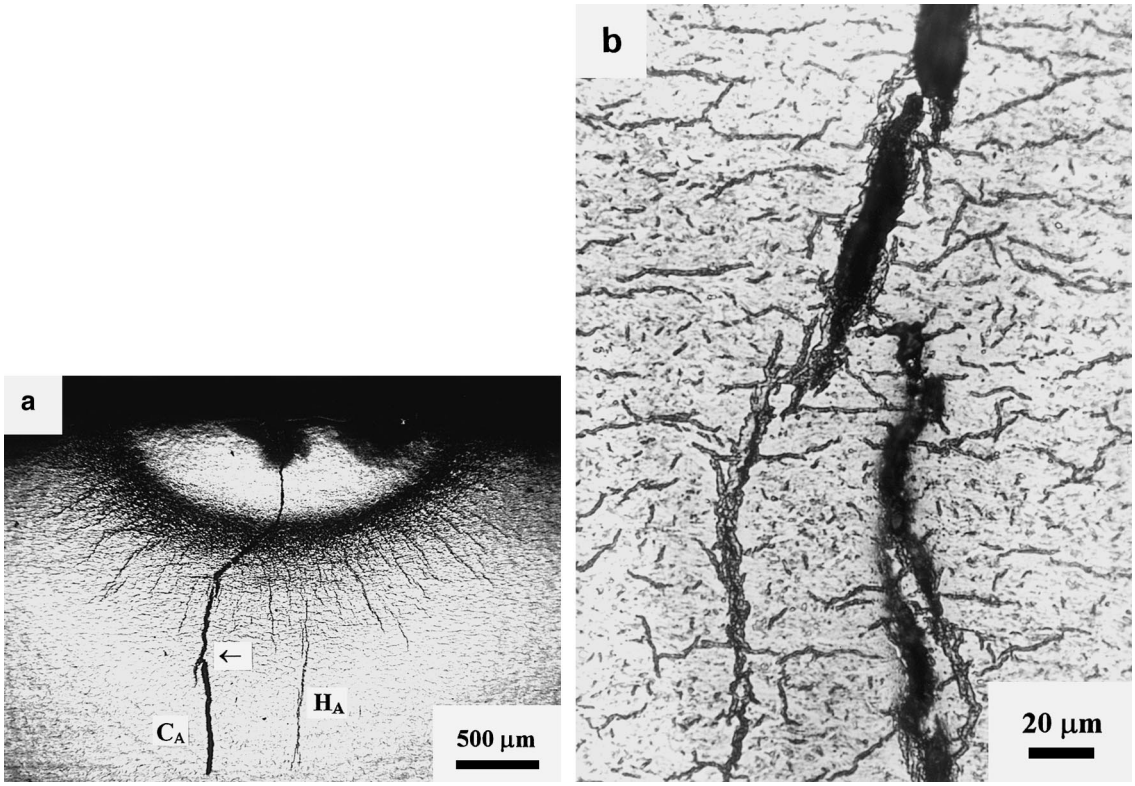

Fig. 9. Micrographs on side A of specimen F after the interruption of the DHC test (940 h). (a) Crack is observed at the left (C_A) and radial hydride string (H_A) at the right. (b) Detail of the crack pointed in (a).

sample F, zones with circumferential hydrides are alternated with radial components zones. This shows that the flattening stresses were not completely relieved by the thermal treatment at 400°C as was observed by Leger and Donner [8]. These residual stresses (about 100 MPa) may increase (tensile zone) or decrease (compressive zone) the total remote stress found by the hydride stacking during its growth.

On the circumferential–axial plane (Fig. 11), crack C_A (observed on side A in Fig. 9) has propagated in the axial direction parallel to the hydride strings. This crack presents (in both planes, circumferential–radial and circumferential–axial) the same stepwise pattern observed at the hydride stackings. Moreover, some hydrides were often found at the initial tip of the crack and overlapped to the preceding crack (Fig. 9(b)). These observations suggest that the crack has possibly advanced along a hydride stacking previously precipitated, similar to the one observed parallel to the crack. Another possibility could be that the crack had propagated by the precipitation of hydride platelets at the crack tip as it was observed in the DHC process by other authors [23, 25]. However, in these works, the hydride particles presented a tapered shape (not observed in sample F) and precipitated just in front of the crack tip but did not overlap as it was shown in the present work. It is interesting to note that the crack observed on side A is quite similar to those cracks found in the blister analysis after the Pickering failure [1,5].

The comparison of results obtained from specimens C and F establishes some differences, which can be explained as follows. The initial non-through-wall crack in sample F and the lower K_I prevented the fracture of the specimen. In this way, the radial hydrides had enough time to grow. In samples *C* (through-wall cracks) the fracture was accomplished in a shorter time compared with sample F. The radial hydrides could have cracked after reaching a critical length and then the cracks could have propagated by the DHC mechanism. The effect of radial hydrides would be mainly an increase of the initial depth of the crack. Additional studies are necessary to elucidate these questions.

4. Conclusions

- When a blister is formed in a Zr–2.5%Nb pressure tube, the stresses produced by the misfit strain are high enough to overcome the threshold stress necessary to precipitate radial hydrides in the matrix. During cooling, hydride plate-

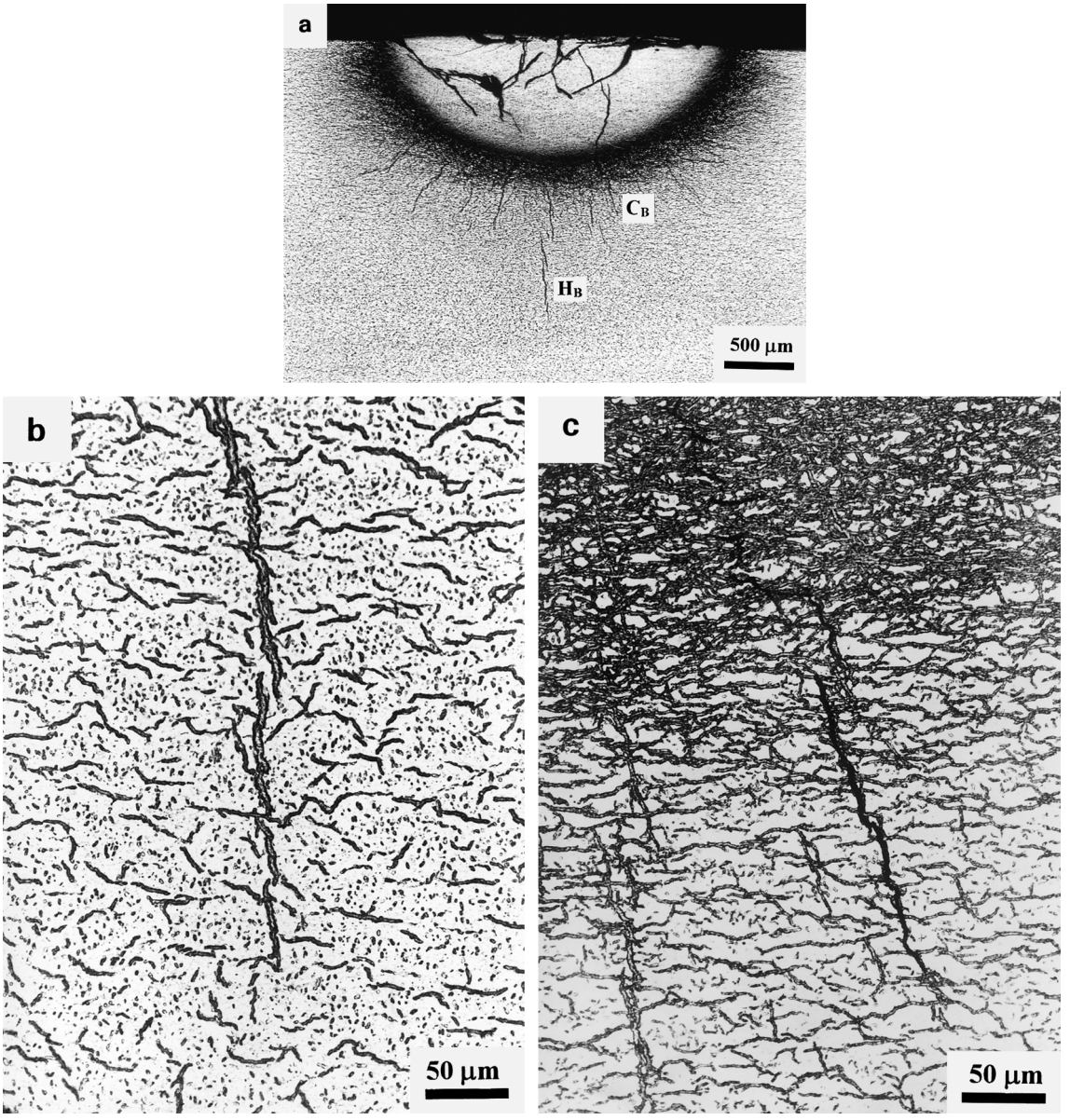

Fig. 10. Micrographs of sample F (after removing 1 mm from side B. (a) A hydride string (H_B) grew in the radial direction of the PT and a crack (C_B) propagated along a hydride radially to the blister. (b) Detail of the radial string of hydrides (H_B) showing the overlapped platelets. (c) Enlarged view of the crack (C_B).

lets are precipitated radially to the blister, even in the absence of external stresses.

- The precipitation of hydrides radially to the blister is favored by a minimum cooling rate, consistent with a hydrogen diffusion controlled process.
- The reach of the zone where these hydrides are precipitated increases as the temperature of the blister growth decreases. An increase of the matrix yield stress and the subsequent increase of the stresses developed around the blister can explain this fact.
- The presence of previous circumferential hydrides around the blister limits the length of radial hydrides but increases their reach.
- When external stresses are applied in the circumferential direction of the PT (DHC test), the blister acts as a stress concentrator. The stress gradient generated around the blister causes hydrogen diffusion (even if no thermal gradient is applied) and the radial hydrides grow in both length and thickness.

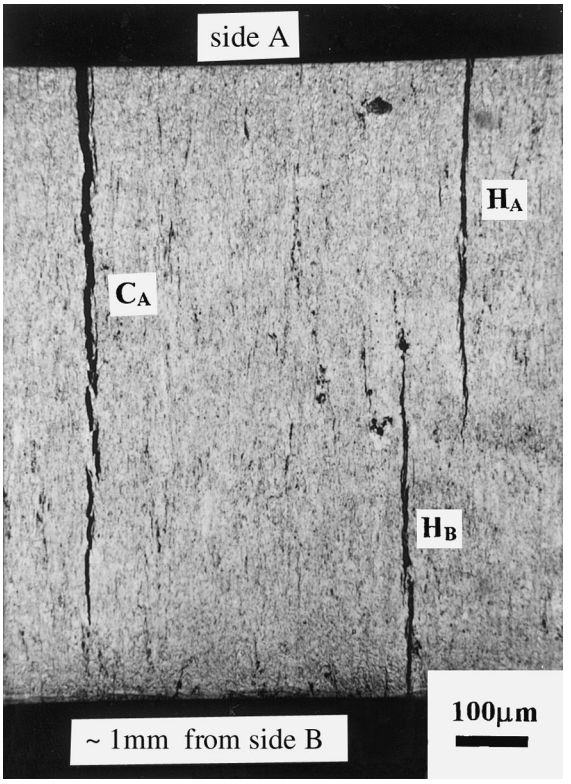

Fig. 11. Specimen F, micrograph of the circumferential–axial section at 1.8 mm from the outer surface of the PT. (C_A) is the crack observed on side A (Fig. 9). H_A and H_B are the radial hydrides observed in Figs. 9 and 10, respectively.

- If a crack originated in a blister crosses the blister-matrix boundary it could propagate inside the matrix along the radial hydrides.
- When the stress concentrator effect of the blister vanishes, the growth of radial hydrides continues by autocatalytic nucleation and by the stress concentrator effect of the hydrides.

Acknowledgements

The authors are specially grateful to Dr M. Ortiz, Dr M. Ipohorski and Dr L. deVedia for many useful discussions.

References

[1] G.J. Field, J.T. Dunn, B.A. Cheadle, Can. Metall. Q. 24 (3) (1985) 181.
[2] M.P. Puls, Metall. Trans. A 19 (1988) 2247.
[3] M. Leger, G.D. Moan, A.C. Wallace, N.J. Watson, ASTM STP 1023, American Society for Testing and Materials, 1989, p. 50.
[4] G. Domizzi, R.A. Enrique, J. Ovejero-García, G.C. Buscaglia, J. Nucl. Mater. 229 (1996) 36.
[5] G.D. Moan, D.K. Rodgers, AECL report No 11106, Ontario, Canada, 1994.
[6] L.A. Simpson, Metall. Trans. A 12 (1981) 2113.
[7] V. Perovic, G.C. Weatherly, C.J. Simpson, Acta Metall. 31 (9) (1983) 1381.
[8] M. Leger, A. Donner, Can. Metall. Q. 24 (3) (1985) 235.
[9] J.W. Christian, The Theory of Transformation in Metals and Alloys, Pergamon, Oxford, 1975, p. 457.
[10] S.-Q. Shi, M.P. Puls, J. Nucl. Mater. 208 (1994) 232.
[11] B.W. Leitch, M.P. Puls, Metall. Trans. A 23A (1992) 797.
[12] G.J.C. Carpenter, J. Nucl. Mater. 48 (1973) 264.
[13] M.L. Vanderglas, Y.J. Kim, Int. J. Pres. Ves. Piping 22 (1986) 177.
[14] Y.J. Kim, M.L. Vanderglas, Trans. ASME 110 (1988) 276.
[15] A.C. Wallace, Ontario Hydro Research Division, Toronto, ON, Canada, Report No 86–175K.
[16] A.C. Wallace, Transactions of the Ninth International Conference on Structural Mechanics in Reactor Tech., 1987, p. 87.
[17] R. Brook, Fracture Mechanics, PMM-A/272, Buenos Aires Argentina, 1979.
[18] Y.P. Chiu, J. Appl. Mech. 44 (1977) 587.
[19] J.J. Kearns, J. Nucl. Mater. 22 (1967) 202.
[20] C.E. Coleman, J.F.R. Ambler, in: Proceedings of the Third International Conference on Zirconium in the Nuclear Industry, Quebec, Canada, 10–12 August 1976, ASTM STP 633.
[21] J.F.R. Ambler, in: Proceedings of the 6th International Conference on Zirconium in the Nuclear Industry, Vancouver, B.C., 28 June–1 July 1982, ASTM STP 824, 1984.
[22] G. Domizzi, G. Vigna, J. Ovejero-García, To be presented at XXVI Reunión Anual de la Asociación Argentina de Tecnología Nuclear, San Carlos de Bariloche, Argentina. 9–12 November 1999.
[23] K. Nuttall, D.P. McCooeye, A.J. Rogowsky, F. Havelock, Scripta Met. 10 (1976) 979.
[24] V. Perovic, G.R. Purdy, L.M. Brown, Acta Metall. 29 (1981) 902.
[25] G.K. Shek, M.T. Jovanovic, H. Seahra, Y. Ma, D. Li, R.L. Eadie, J. Nucl. Mater. 231 (1996) 221.